Results in Physics 8 (2018) 352–356

Contents lists available at ScienceDirect

Results in Physics

journal homepage: www.journals.elsevier.com/results-in-physics

Near-infrared optical properties of Yb^{3+}-doped silicate glass waveguides prepared by double-energy proton implantation

Xiao-Liang Shen [a], Qi-Feng Zhu [a], Rui-Lin Zheng [a], Peng Lv [a], Hai-Tao Guo [b], Chun-Xiao Liu [a,*]

[a] College of Electronic and Optical Engineering & College of Microelectronics, Nanjing University of Posts and Telecommunications, Nanjing 210023, China
[b] State Key Laboratory of Transient Optics and Photonics, Xi'an Institute of Optics and Precision Mechanics, Chinese Academy of Sciences (CAS), Xi'an 710119, China

ARTICLE INFO

Article history:
Received 17 November 2017
Received in revised form 15 December 2017
Accepted 15 December 2017
Available online 19 December 2017

Keywords:
Waveguide
Yb^{3+}-doped silicate glasses
Ion implantation

ABSTRACT

We report on the preparation and properties of an optical planar waveguide structure operating at 1539 nm in the Yb^{3+}-doped silicate glass. The waveguide was formed by using (470 + 500) keV proton implantation at fluences of $(1.0 + 2.0) \times 10^{16}$ ions/cm^2. The waveguiding characteristics including the guided-mode spectrum and the near-field image were investigated by the m-line technique and the finite-difference beam propagation method. The energy distribution for implanted protons and the refractive index profile for the proton-implanted waveguide were simulated by the stopping and range of ions in matter and the reflectivity calculation method. The proton-implanted Yb^{3+}-doped silicate glass waveguide is a candidate for optoelectronic elements in the near-infrared region.

Introduction

Optical waveguides play an important role in the development of optoelectronics and integrated optics. They are the transmission channels for signal propagation and the interconnections between different optical devices. Therefore, the fabrication of waveguide structures and investigation on their characteristics have become more and more attractive in the last decades [1–5]. Ion implantation [6], ion exchange [7], thin film deposition [8] and femtosecond laser inscription [9] are the most commonly used techniques for the manufacture of optical waveguides in a variety of optical materials. Comparing with other ways, the method of ion implantation possesses its unique advantages, owing to its easiness to control the concentration and depth of the implanted ions [10,11]. Furthermore, the structural parameters of an ion-implanted optical waveguide including the thickness of the core layer and the refractive index profile are mainly dependent on the concentration and the depth of the implanted ions [12–14]. The energetic carbon and oxygen ions, as well as protons, have usually been employed to produce waveguide structures. However, the penetration depth of the proton implantation is much deeper than that of the heavy-ion implantation (such as O^{2+} and C^{+}) for the same implanted energy, since hydrogen is the lightest among all the elements. This fact is especially advantageous for the proton implantation when the light with near-infrared wavelength propagates in optical waveguides. In view of these merits, the proton implantation method has been chosen to fabricate optical waveguides in the present work.

For the construction of high-quality waveguides, a suitable matrix material is another important factor besides the preparation method [15]. Yb^{3+}-doped silicate glasses have emerged in recent years as gain media for the next generation nuclear fusion and high-power lasers. They exhibit broad absorption and emission band, and high emission section. Meanwhile, the concentration quenching and excited-state absorption can be avoided to some extent, owing to the two manifolds (the ground $^2F_{7/2}$ state and the excited $^2F_{5/2}$ state). Yb^{3+}-doped silicate glasses show their own benefits such as possible fused coupling with silica fiber and low cost over the counterparts including Yb^{3+}-doped borate and phosphate glasses. Therefore, Yb^{3+}-doped silicate glasses are ideal as target substrate for the preparation of optical planar waveguides [16–19].

In the past few years, several reports have been communicated for ion-implanted waveguides in silicate glasses doped with Yb^{3+} rare earth ions. For example, channel waveguides in Yb^{3+}-doped silicate glasses have been manufactured by triple-energy helium-ion implantation with a standard photolithographic technique and planar waveguides have been formed by low-dose carbon ion implantation in the Yb^{3+}-doped silicate glasses [20,21]. In particular, the technique of the proton implantation has been applied to manufacture the optical waveguide structure in the Yb^{3+}-doped silicate glass [22]. The features of the waveguides are all investigated in visible (632.8 nm) region. However, optical waveguide

* Corresponding author.
E-mail address: cxliu0816@sina.com (C.-X. Liu).

https://doi.org/10.1016/j.rinp.2017.12.040
2211-3797/

devices operated in the telecommunication windows around ~1.5 μm are indispensable in functional optical-communication networks [23]. Therefore, it is necessary to explore 1.5-μm ion-implanted Yb^{3+}-doped silicate glass waveguides. In the present work, we fabricated waveguide structures by means of the double-energy proton implantation with energies of (470 + 500) keV and doses of $(1.0 + 2.0) \times 10^{16}$ ions/cm^2 and focused on their near-infrared (1539 nm) optical properties.

Experiments

Yb^{3+}-doped silicate glasses in the system of $65SiO_2$-$10B_2O_3$-$4Al_2O_3$-$7Na_2O$-$6La_2O_3$-$6Y_2O_3$-$2Yb_2O_3$ were synthesized by the standard melt-quenching method. A 500 g mixture of raw materials with high purity were added successively into a platinum crucible placed in an electrical resistance furnace and melt at 1150 °C for 2 h. The glass melt was stirred, clarified and homogenized for 4 h after the temperature of the electric furnace rose to 1300 °C. Then, the melt was poured onto a preheated brass mold and annealed at T_g (Transformation temperature) in a muffle furnace.

The as-prepared Yb^{3+}-doped silicate glass was cut and polished into some wafers with 10.0 mm length, 10.0 mm width and 2.0 mm thickness. The wafers were carefully cleaned before any optical measurement. The photoluminescence spectrum and the fluorescence lifetime of the Yb^{3+}-doped silicate glass were measured by an Edinburgh FLS920P spectrometer (Edinburgh, UK) with a 980-nm diode laser for excitation. The optical absorption spectrum in the 400–1600 nm wavelength range was collected by a JASCO U-570 UV–VIS-NIR spectrophotometer and its refractive index was measured by the m-line prism coupling method at a wavelength of 1539 nm.

The ion implantation was performed in the Institute of Semiconductors of CAS on an ion-implantor. As well known, a double-energy ion implantation could broaden the width of the optical barrier, resulting in reduction of the light leakage from the optical waveguide. Therefore, 470-keV proton implantation with a fluence of 1×10^{16} ions/cm^2 and 500-keV H^+ ion implantation with a dose of 2×10^{16} ions/cm^2 were irradiated successively on the same Yb^{3+}-doped silicate glass.

The optical propagation properties of the as-implanted Yb^{3+}-doped silicate glass were characterized by the dark-mode spectroscopy with the Metricon model 2010 prism coupler at 1539 nm. The light intensity on the photodetector would fluctuate when the incident angle was continuously adjusted in the measurement procedure. At some discrete angles, the incident light at the prism/sample interface would tunnel through the small air gap between the prism and the sample into the waveguide, resulting in a dip at the photodetector.

Results and discussion

Fig. 1(a) shows the fluorescence spectrum of the Yb^{3+}-doped silicate glass in the range from 900 nm to 1200 nm. Besides a main peak caused by some incompletely filtered laser emission at 977 nm, there is a sub peak around 1008 nm, which is attributed to the $^2F_{5/2} \rightarrow {}^2F_{7/2}$ transition of the ytterbium ion emission. Fig. 1 (b) depicts the time decay curve of the photoluminescence intensity at 1008 nm for the $^2F_{5/2} \rightarrow {}^2F_{7/2}$ transition. The fluorescence lifetime of the metastable level ($^2F_{5/2}$) in the Yb^{3+}-doped silicate glass is calculated to be about 407 μs, which is obtained by fitting the fluorescence decay curve with the single-exponential function.

Fig. 2(a) shows the transmittance spectrum of the Yb^{3+}-doped silicate glass with a thickness of 2.0 mm. The transparent ratio is relatively high and even more than 85% in the wavelength ranges of 400–850 nm and 1100–1600 nm. A sharp absorption band centered at 978 nm was observed, owing to the transition of Yb^{3+} ions from the $^2F_{7/2}$ ground-state level to the $^2F_{5/2}$ excited-state level. Fig. 2(b) illustrates the refractive index of the Yb^{3+}-doped silicate glass at a wavelength of 1539 nm. The substrate refractive index is 1.5982, as the dashed line represented.

The nuclear energy loss in the ion implantation process is supposed to be an origin of the displacement and the damage in the irradiated region. It is simulated by the stopping and range of ions in matter code (SRIM 2013) [24] for the 470-keV and 500-keV proton implantation into the Yb^{3+}-doped silicate glass, as Fig. 3 shown. The 470-keV proton implantation results in the maximal nuclear energy loss of 1.16 keV/μm at the depth of 5.90 μm. For the 500-keV implantation of the protons, the maximum of the nuclear energy deposition is about 1.14 keV/μm at 6.36 μm beneath the glass surface. The depth-distribution of the nuclear energy losses for the double-energy proton irradiation are calculated as simple algebraic sums of the corresponding pairs of single-energy proton distributions. Therefore, a peak of 1.73 keV/μm with a width of 0.07 μm is observed at about 6.0 μm from the glass surface in Fig. 3.

The cross-sectional photograph of the Yb^{3+}-doped silicate glass after the proton irradiation was recorded by an optical microscopy in transmission mode, as Fig. 4 shown. The area between the two dashed lines is the waveguide layer, which is a smooth strip in Fig. 4. The thickness of the optical structure is about 6.0 μm and close to the depth-distribution of the nuclear energy losses for the (470 + 500) keV proton implantation into the Yb^{3+}-doped silicate glass.

Fig. 5 shows the measured relative intensity of the light with a wavelength of 1539 nm reflected from the rutile prism of the prism-coupling system (Metricon Model 2010 prism coupler) as a function of the effective refractive index for the optical planar waveguide formed by (470 + 500) keV proton implantation at doses of $(1.0 + 2.0) \times 10^{16}$ ions/cm^2 in the Yb^{3+}-doped silicate glass through the *m*-line method. As shown in Fig. 5, there are two dips in the dark-mode spectrum. The number of dips at 1539 nm is one less than that of the 632.8-nm m-line curve in the previous report [22]. Compared with the second dip, the first one is relatively sharp and deep. Therefore, the first dip maybe correspond to a propagation mode and the second one would present a leaky mode. The effective refractive indices of the two dips are 1.5972 and 1.5775, which are both less than the refractive index of the substrate (1.5982). It suggests that the refractive index of the waveguide layer is lower than the substrate refractive index.

The refractive index profile of an optical waveguide has an influence on both the propagation modes and the actual applications. The reflectivity calculation method (RCM) can be used to fit the refractive index distribution of an ion-implanted optical waveguide based on its *m*-line curve [25,26]. Fig. 6 shows the refractive index profile of the proton-implanted waveguide in the Yb^{3+}-doped silicate glass by means of the RCM. It is a typical barrier-confined distribution. The refractive index in the waveguide region is 1.5967 at 1539 nm, which is about 0.0015 less than the refractive index of the pure glass matrix. There is a large negative index change of -0.012 at a depth of 6.0 μm that is consistent with the peak position of the nuclear energy loss in Fig. 3. In addition, the effective refractive indices of the theoretical modes for the RCM-reconstructed distribution of refractive index are 1.5933 and 1.5813. As one can see, the differences between the measured and simulated effective refractive indices for the same mode are in the order of 10^{-3}.

The FD-BPM (finite-difference beam propagation method) is a well-known technique for the simulation of the near-field intensity distributions in a large number of waveguide devices including couplers and splitters [27,28]. Fig. 7 shows the FD-BPM-simulated optical image at a wavelength of 1539 nm in the waveguide formed by the proton implantation in the Yb^{3+}-doped silicate

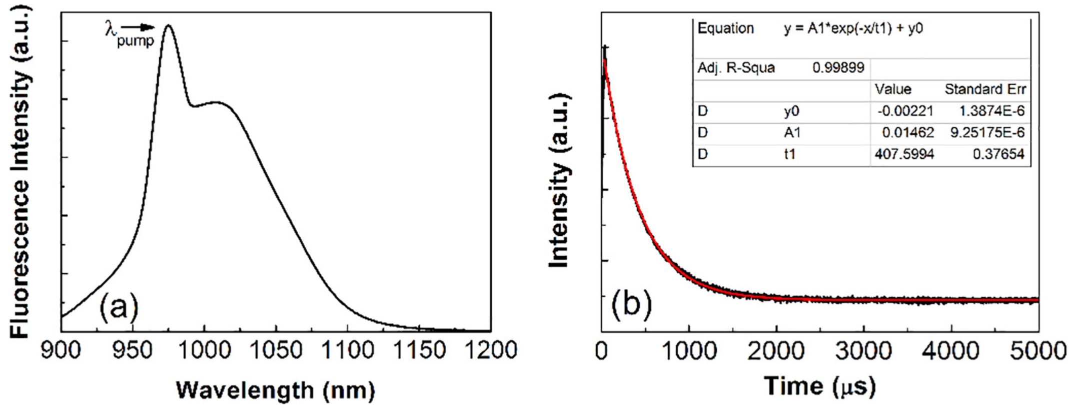

Fig. 1. (a) Photoluminescence spectrum and (b) lifetime curve of the Yb^{3+}-doped silicate glass.

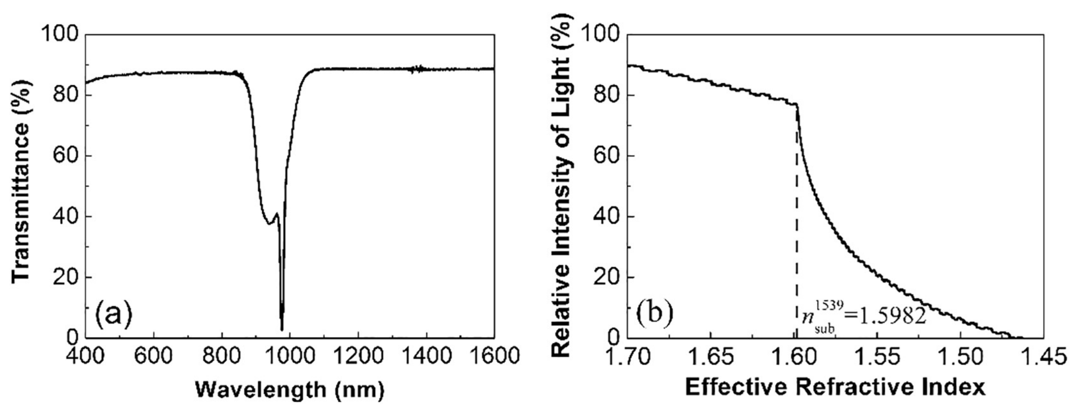

Fig. 2. (a) Transmission spectrum and (b) refractive index of the Yb^{3+}-doped silicate glass.

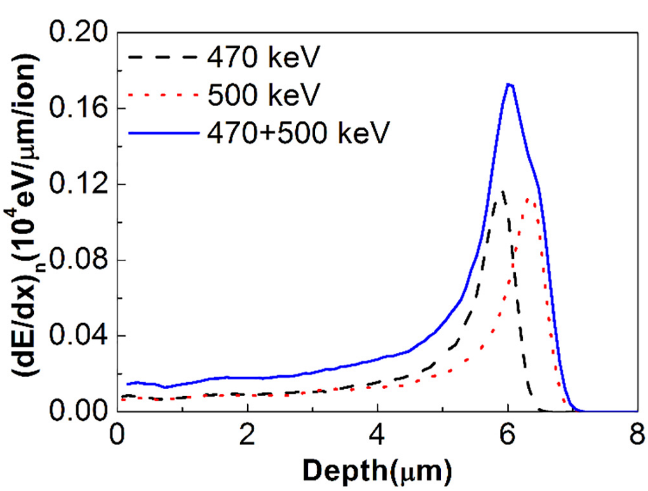

Fig. 3. Nuclear energy losses for the 470 (dash line), 500 (dot line) and 470 + 500 (solid line) keV proton implantation into the Yb^{3+}-doped silicate glass.

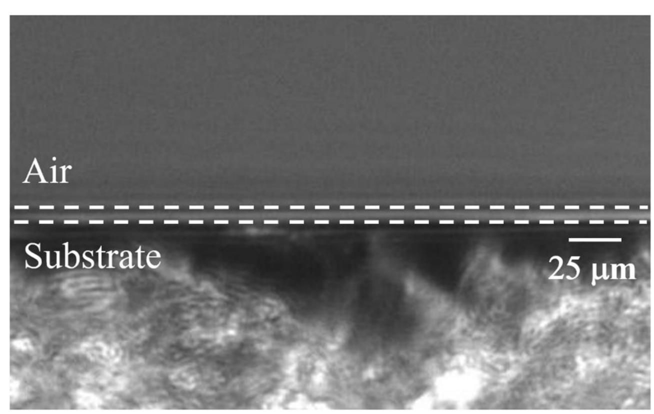

Fig. 4. Cross-sectional image of the proton-implanted Yb^{3+}-doped silicate glass.

glass. The shape of the computed transverse mode pattern is similar to the cross-sectional microscopy image of the waveguide. Especially, the width of the simulated pattern in the vertical direction approximatively equals to the thickness of the proton-implanted glass waveguide. As one can see, the light from the output face of the waveguide structure is uniform and continuous. Furthermore, there is no light leakage phenomenon. It means that the light at 1539 nm can be well confined in the vertical direction in the proton-implanted Yb^{3+}-doped silicate glass waveguide. In addition, the calculated effective refractive index of the TE_0 mode based on the FD-BPM is 1.595984 at 1539 nm and is close to the counterpart in the dark-mode spectrum (1.5972 in Fig. 5).

Conclusion

A waveguide structure has been prepared by the double-energy implantation of protons in the Yb^{3+}-doped silicate glass. Its optical properties have been studied at 1539 nm. The fundamental propagation mode can be contained in the waveguide, according to the dark-mode spectrum. The refractive index in the waveguide layer

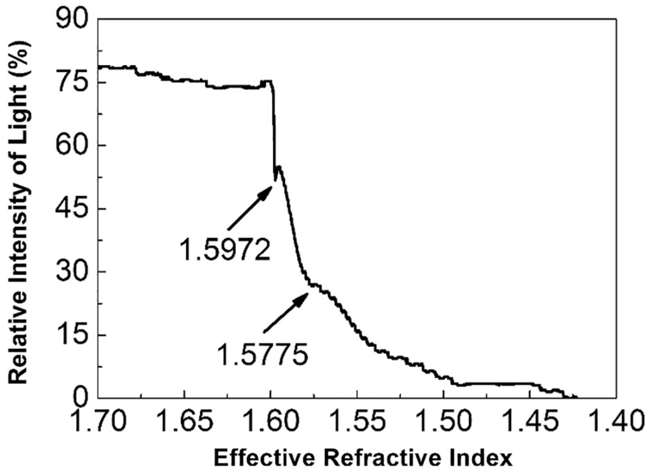

Fig. 5. Dark-mode spectroscopy at 1539 nm for the Yb^{3+}-doped silicate glass waveguide fabricated by the double-energy proton implantation.

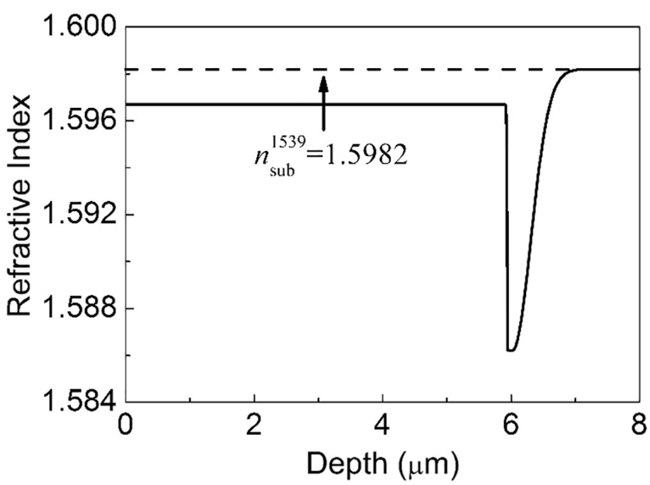

Fig. 6. Refractive index profile at 1539 nm for the double-energy proton-implanted Yb^{3+}-doped silicate glass waveguide.

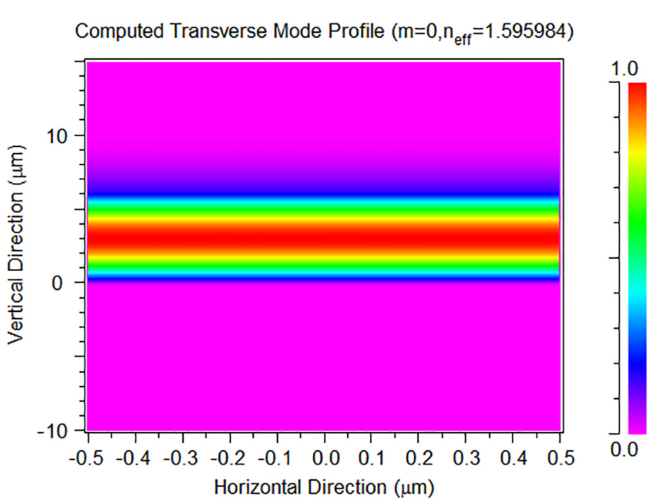

Fig. 7. Calculated near-field intensity pattern of the proton-implanted waveguide in Yb^{3+}-doped silicate glass at 1539 nm.

is 0.0105 more than the minimum index of the optical barrier. The FD-BPM calculated near-field light intensity distribution suggests that the 1539-nm light can propagate in the optical structure. The proton-implanted Yb^{3+}-doped silicate glass waveguides have the potential to act as diverse photonic devices for optical communications.

Acknowledgements

The authors acknowledge the support from National Natural Science Foundation of China (Grant Nos. 11405041 and 61475189), Natural Science Foundation of Jiangsu Province (Grants BK2014042609), and Scientific Research Starting Foundation for New Teachers of Nanjing University of Posts and Telecommunications (NUPTSF) (Grant No. NY214159).

Appendix A. Supplementary data

Supplementary data associated with this article can be found, in the online version, at https://doi.org/10.1016/j.rinp.2017.12.040.

References

[1] Kip D. Photorefractive waveguides in oxide crystals: fabrication, properties, and applications. Appl Phys B 1998;67:131–50.
[2] Ríos C, Stegmaier M, Hosseini P, Wang D, Scherer T, Wright CD, Bhaskaran H, Pernice WHP. Integrated all-photonic non-volatile multi-level memory. Nature Photon 2015;9:725–32.
[3] Hu H, Ricken R, Sohler W. Low-loss ridge waveguides on lithium niobate fabricated by local diffusion doping with titanium. Appl Phys B 2010;98:677–9.
[4] Wang L, Haunhorst CE, Volk MF, Chen F, Kip D. Quasi-phase-matched frequency conversion in ridge waveguides fabricated by ion implantation and diamond dicing of MgO: $LiNbO_3$ crystals. Opt Express 2015;23:30188–94.
[5] Wang XL, Wang KM, Fu G, Li SL, Shen DY, Ma HJ, Nie R. Low propagation loss of the waveguides in fused quartz by oxygen ion implantation. Opt Express 2004;12:4675–80.
[6] Chen F. Construction of two-dimensional waveguides in insulating optical materials by means of ion beam implantation for photonic applications: fabrication methods and research progress. Crit Rev Solid State 2008;33:165–82.
[7] Tervonen A, West BR, Honkanen S. Ion-exchanged glass waveguide technology: a review. Opt Eng 2011;50:071107.
[8] Eason RW, May-Smith TC, Sloyan KA, Gazia R, Darby MSB, Sposito A, Parsonage TL. Multi-beam pulsed laser deposition for advanced thin-film optical waveguides. J Phys D Appl Phys 2014;47:034007.
[9] Chen F, Vázquez de Aldana JR. Optical waveguides in crystalline dielectric materials produced by femtosecond-laser micromachining. Laser Photon Rev 2014;8(2):251–75.
[10] Stanek S, Nekvindova P, Svecova B, Vytykacova S, Mika M, Oswald J, Mackova A, Malinsky P, Spirkova J. The influence of silver-ion doping using ion implantation on the luminescence properties of Er-Yb silicate glasses. Nucl Instrum Methods Phys Res B 2016;371:350–4.
[11] Tan Y, Chen F, Wang L, Jiao Y. Carbon ion-implanted optical waveguides in Nd: $YLiF_4$ crystal: refractive index profiles and thermal stability. Nucl Instrum Methods Phys Res B 2007;260:567–70.
[12] Bányász I, Zolnai Z, Fried M, Berneschi S, Pelli S, Nunzi-Conti G. Leaky mode suppression in planar optical waveguides written in Er:TeO_2-WO_3 glass and CaF_2 crystal via double energy implantation with MeV N^+ ions. Nucl Instrum Methods Phys Res B 2014;326:81–5.
[13] Vázquez GV, Valiente R, Gómez-Salces S, Flores-Romero E, Rickards J, Trejo-Luna R. Carbon implanted waveguides in soda lime glass doped with Yb^{3+} and Er^{3+} for visible light emission. Opt Laser Technol 2016;79:132.
[14] Tan Y, Zhang C, Chen F, Liu FQ, Jaque D, Lu QM. Room-temperature continuous wave laser oscillations in Nd:YAG ceramic waveguides produced by carbon ion implantation. Appl Phys B 2011;103:837–40.
[15] Liu CX, Fu LL, Cheng LL, Zhu XF, Lin SB, Zheng RL, Zhou ZG, Guo HT, Li WN, Wei W. Optimization effect of annealing treatment on oxygen-implanted Nd:CNGG waveguides. Mod Phys Lett B 2016;30:1650261.
[16] Boulon G. Why so deep research on Yb^{3+}-doped optical inorganic materials? J Alloy Compd 2008;451:1–11.
[17] Agnesi A, Carrà L, Di Marco C, Piccoli R, Reali G, Tartara L. Characterization of tunable low power Yb-doped fiber CW oscillators. Opt Laser Technol 2012;44:1437–41.
[18] Peng B, Jiang L, Qiu XM, Fan ZC, Huang W. Ytterbium doped heavy metal oxide glasses with high emission cross-section. J Alloy Compd 2005;398:170–2.
[19] Jaque D, Lagomacini JC, Jacinto C, Catunda T. Continuous-wave diode-pumped Yb: glass laser with 90% slope efficiency. Appl Phys Lett 2006;89:121101–3.
[20] Liu CX, Cheng S, Zhao JH, Li WN, Wei W, Peng B, Guo HT. Monomode optical planar and channel waveguides in Yb^{3+}- doped silicate glasses formed by helium ion implantation. Opt Laser Technol 2013;52:10–4.

[21] Liu CX, Cheng S, Li WN, Wei W, Peng B. Monomode optical waveguides in Yb^{3+}-doped silicate glasses produced by low-dose carbon ion implantation. Jpn J Appl Phys 2012;51:052601.
[22] Liu CX, Cheng S, Guo HT, Li WN, Liu XH, Wei W, Peng B. Proton-implanted optical planar waveguides in Yb^{3+}-doped silicate glasses. Nucl Instrum Methods Phys Res B 2012;289:18–21.
[23] Bradley JDB, Pollnau M. Erbium-doped integrated waveguide amplifiers and lasers. Laser Photon Rev 2011;5(3):368–403.
[24] J.F. Ziegler, SRIM-the stopping and range of ions in matter, http://www.srim.org.
[25] Chandler PJ, Lama FL. A new approach to the determination of planar waveguide profiles by means of a nonstationary mode index calculation. Opt Acta 1986;33:127–43.
[26] Tan Y, Chen F, Wang L, Wang KM, Lu QM. Thermal stability of carbon-ion-implanted Nd:YVO_4 optical planar waveguide. J Korean Phys Soc 2008;52:S80–3.
[27] Rsoft Design Group, Computer software BeamPROP version 8.0, http://www.rsoftdesign.com.
[28] Tan Y, Vázquez de Aldana JR, Chen F. Femtosecond laser written lithium niobate waveguide laser operating at 1085 nm. Opt Eng 2014;53:107109.